

## Mechanical and Thermal Degradation Properties of Silk from African Wild Silkmoths

Addis Teshome,<sup>1,2</sup> John M. Onyari,<sup>2</sup> Suresh K. Raina,<sup>1</sup> Jacques M. Kabaru,<sup>2</sup> Fritz Vollrath<sup>3</sup>

<sup>1</sup>ICIPE—African Insect Science for Food and Health, Environmental Health Division, Nairobi 30772-00100, Kenya

<sup>2</sup>School of Physical Sciences and School of Biological Sciences, University of Nairobi, Nairobi 30197-00100, Kenya

<sup>3</sup>Silk Research Group, Department of Zoology, University of Oxford, Oxford OX1 3PS, United Kingdom

Correspondence to: A. Teshome (E-mail: additi09@gmail.com or akebede@icipe.org)

**ABSTRACT:** Variations among silk of four African wild silkmoths, *Argema mimosae*, *Anaphe panda*, *Gonometa postica*, and *Epiphora bauhiniae*, was studied regarding their mechanical properties and thermal degradation behaviors. Cocoon shells and individual degummed fibers were examined using tensile testing, thermogravimetric analysis, and scanning electron microscope (SEM). *A. mimosae* and *G. postica* cocoon shells had marginally higher initial moduli and strains at maximum stress. The stress–strain curves of *Bombyx mori* and *A. panda* degummed fibers lacked clear yielding points. *G. postica* fibers had the highest breaking energy (76.4 J/cm<sup>3</sup>) and breaking strain (41.3%). The ultimate tensile strength was the highest for *B. mori* (427 MPa). Fiber pull-out and detachment was predominant in fracture surfaces of both the cocoon shells and the fibers. Wild cocoon shells and degummed fibers had higher temperature for dehydration loss than *B. mori*. *A. mimosae* fibers (11.9%) and *G. postica* cocoon shells (13.3 %) had the highest weight loss due to dehydration. *E. bauhiniae* cocoon shells and *B. mori* fibers had the highest total weight losses of 97.2 and 93.4%, respectively. The African silks exhibited variations in their mechanical and thermal degradation properties related to their physical and chemical structure and composition. © 2012 Wiley Periodicals, Inc. *J. Appl. Polym. Sci.* 000: 000–000, 2012

**KEYWORDS:** degradation; yielding; fibers; fracture; thermal properties

Received 15 December 2011; accepted 13 April 2012; published online

DOI: 10.1002/app.37873

### INTRODUCTION

Natural fibers from animals and plants are gaining increasingly in importance, once again. Silk is a unique class of structural animal fiber and has long been regarded as a superb natural material due to its characteristic high strength, elongation, feel, and luster.<sup>1</sup> The variation in composition, structure, and properties of silks from different arthropods has led to its considerations in wider applications expanding from more traditional textile industries to fields such as biomedical, biotechnological, and tissue engineering. The usefulness of silk fibers in these and many other applications is associated with its predominant failure mechanism under the conditions of the application and its adaptability to varied environmental conditions facilitated by the silk's molecular composition and hierarchical structure. These, in turn, are both affected by the conditions during its production such as spinning speed, relative humidity, temperature, pH, ionic strength, solvent composition, and mechanical stress as well as the degumming process.<sup>2–5</sup> The mechanical properties of silk fibers also depend on the structure of the silk

constituent proteins (sericin and fibroin) before and after silk fiber formation.<sup>6</sup> For example, sericin coating can add to the tensile properties of silk fibers, although these are primarily determined by their fibroin structure.<sup>7</sup> Sericin might also affect the transition of silk fibroin from the random coil or  $\alpha$ -helix to the  $\beta$ -sheet structure and further improve the mechanical properties of silk fibroin fibers.<sup>8</sup> High crystallinity confers the silk material greater strength by virtue of the network of hydrogen bonds between and within the proteins.<sup>9</sup>

Temperature and moisture are among the environmental stresses influencing properties and functions of silk cocoons and fibers. Cocoon shells are important in temperature regulation, water loss reduction from the pupae, and acquisition of heat.<sup>10</sup> Temperature also influences the amount of water absorbed by silk fibers resulting in alteration of physical properties. Chemical composition and structure of silk fibers determine the thermal tolerance behavior of the cocoon shells and fibers and the resulting weight loss due to dehydration and/or decomposition. Hence, it is appropriate to deploy Thermal Analysis to

© 2012 Wiley Periodicals, Inc.

**Table I.** Tensile Properties of Cocoon Shells of *A. mimosae*, *G. postica*, and *B. mori*

Species	Initial modulus (MPa)	Maximum stress (MPa)	Strain at Max stress (%)	Breaking energy (J/cm <sup>3</sup> )
<i>A. mimosae</i>	404.6 ± 59.8a	69.6 ± 7.0c	21.2 ± 1.0a	13.8 ± 1.9b
<i>G. postica</i>	397.4 ± 63.4a	47.2 ± 1.7b	23.3 ± 1.2a	11.4 ± 0.6b
<i>B. mori</i>	334.5 ± 28.3a	101.1 ± 4.2a	20.8 ± 1.2a	20.1 ± 0.7a

Means followed by the same letter in the same column are not statistically significant ( $P > 0.001$ ) according to least significant difference (LSD) test.

investigate the response of natural materials to temperature scans and to explore together with other data, the structure–property–function relations of natural cocoons.<sup>11</sup> Accordingly, we set out to explore in a comparative study the mechanical properties and thermal degradation behavior patterns of cocoon shells and degummed fibers from four African wild silkmoths.

## MATERIALS AND METHODS

### Mechanical Properties of Cocoon Shells

Cocoon shells of two African wild silkmoths, *Gonometa postica* and *Argema mimosae*, were selected because of their single cocoon shell structure. *Bombyx mori* (Race *icipe* II) obtained from the Commercial Insects Programme, International Centre of Insect Physiology and Ecology (*icipe*) were also used for comparison. Five cocoon shells were used for each species. Two full cocoon shell strips (dimensions of 5 × 15 mm<sup>2</sup>) were cut longitudinally from each cocoon from the middle sections. Instron 5542 tensile testing instrument (500-N load cell) was used for tensile testing and all tests were carried out at room temperature with gauge length of 5 mm and at a speed of 2 mm/min.

### Mechanical Properties of Single Fibers

Cleaned cocoon shells were degummed by boiling with 5 g/L of Na<sub>2</sub>CO<sub>3</sub> solution for 1 (*B. mori*), 1.5 (*G. postica*), 3 (*Epiphora bauhiniiae* and *A. mimosae*), and 5 h (*Anaphe panda*). Boiled cocoons were soaked in star soft solution of 50 mL/L of distilled water for 3 min and washed twice with hot and cold distilled water. Fibers of 100-mm long were obtained by pulling gently and were allowed to dry overnight in air before testing. Silk fibers were cut gently into 30 mm to make sure that the fibers were not stressed plastically during the process. Before being tested, each specimen was examined under an optical microscope to ensure that only single fibers were used. Every cut fiber was then mounted and taped across a hole, which is 10-mm long, of a rectangular cardboard that was then fixed in an Instron machine. Cardboards were cut on both sides and separated

into two parts to ensure tensile loading was completely transmitted to the fiber during test. All tests were conducted at gauge length of 10 mm and speed of 0.1 mm/s at 22°C and 55% relative humidity. Ten tests were made for each species to generate the average tensile stress–strain curve. The tensile parameters were calculated with a home designed program in Excel (Tensile Import v2.0). The J-integral method was used to determine the energy to break. Stress–strain curves were plotted using Origin Pro 8. SAS (SAS institute 2010) was used for statistical analysis of the data with one-way analysis of variance (ANOVA). Cross-sectional areas of the fibers were prepared by clamping orientated silk threads in a holder and cutting them across with a new razor blade before sputtering them with gold (JEOL JFC-1100E ion sputter) and viewed under SEM (JEOL Neoscope JCM-5000 (Nikon, UK)). Digital images of transverse sections on SEM micrographs were manually circled and analyzed with ImageJ 1.42q. Normalized cross-sectional areas were obtained by averaging 50 brins for each sample assuming that sample volume is conserved during the tensile tests.<sup>12</sup>

### Fractography Analysis

Cocoon shells and fibers after the tensile failure were analyzed by SEM to investigate the fracture mechanism.

### Thermogravimetric Analysis

Disks of cocoon shell and degummed fibers (7-mm diameter) were pressed out from middle section of the cocoon and compressed degummed floss, respectively, with a sharp hole-punch. The samples were loaded into a Q500 thermogravimetric analysis (TGA) from thermal analysis (TA) instruments. The samples were scanned from room temperature to 900 and 800°C for cocoon shells and degummed fibers, respectively, at a heating rate of 20°C/min, N<sub>2</sub> flow of 60 mL/min and air cool time of 40 min. Five tests were made for each species, and results were averaged. Samples of cocoon shell and degummed fiber disks after thermogravimetric analysis (TGA) were viewed under SEM.

**Table II.** Tensile Properties of Single Degummed Silk Fibers

Species	Initial modulus (MPa)	Ultimate tensile strength (MPa)	Ultimate tensile strain (%)	Breaking energy (J/cm <sup>3</sup> )
<i>A. panda</i>	6344.4 ± 798.9b	365.1 ± 51.1ab	17.7 ± 0.7c	43.3 ± 7.2cd
<i>A. mimosae</i>	8326.5 ± 742.0a	363.4 ± 6.5ab	20.7 ± 1.0bc	51.6 ± 2.9bc
<i>E. bauhiniiae</i>	7497 ± 331.7ab	247.7 ± 6.3c	20.8 ± 1.3b	34.5 ± 2.4d
<i>G. postica</i>	7153.9 ± 544.6ab	310 ± 37.1b	41.3 ± 1.4a	76.4 ± 8.2a
<i>B. mori</i>	8787 ± 555.1a	427.6 ± 10.6a	21.8 ± 0.5b	66 ± 2.8ab

Means followed by the same letter in the same column are not statistically significant ( $P > 0.001$ ) according to LSD test.

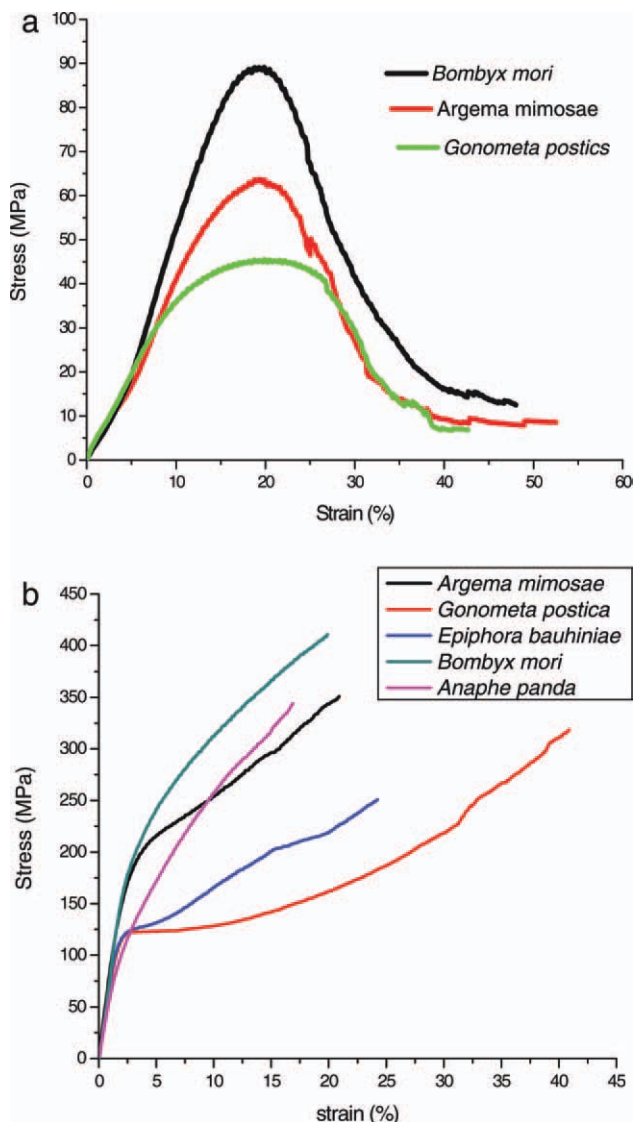


**Figure 1.** Stress–strain curves of cocoon shells and degummed fibers. [Color figure can be viewed in the online issue, which is available at [wileyonlinelibrary.com](http://wileyonlinelibrary.com).]

**Table III.** Cross-Sectional Area of Single Silk Fibers (Brin) and Thickness of Cocoon Shell Walls

Species	Area ( $\mu\text{m}^2$ )	n	Cocoon shell thickness (mm)	n
<i>A. panda</i>	$96.7 \pm 5.7c$	50	$0.379 \pm 0.01b$	50
<i>A. mimosae</i>	$388.5 \pm 14.5a$	50	$0.234 \pm 0.01d$	50
<i>E. bauhiniae</i>	$100.4 \pm 5.3c$	50	$0.318 \pm 0.008c$	50
<i>G. postica</i>	$160.8 \pm 6.8b$	50	$0.536 \pm 0.008a$	50
<i>B. mori</i>	$60.2 \pm 2.1d$	50	$0.207 \pm 0.008e$	50

Means followed by the same letter in the same column are not statistically significant ( $P > 0.001$ ) according to LSD test.

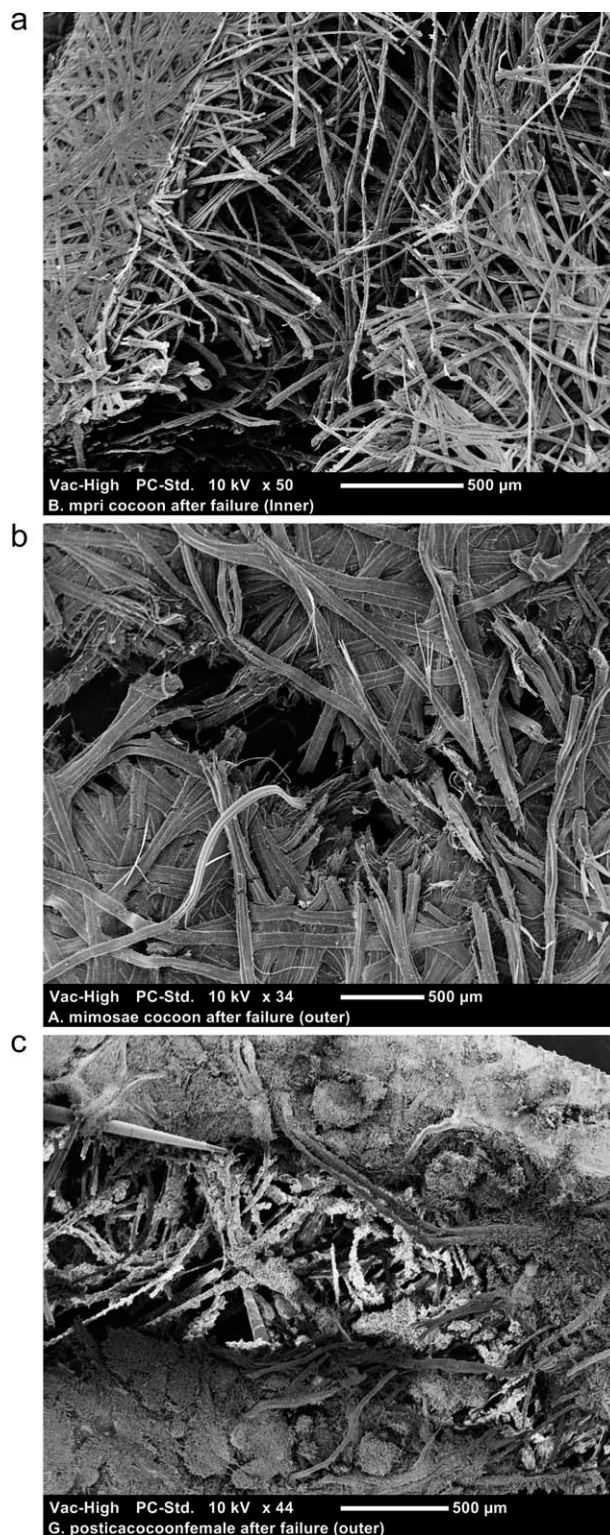


**Figure 2.** SEM micrographs of fracture surfaces of cocoon shells after tensile failure.

## RESULTS

### Mechanical Properties

The measured data of the tensile properties of cocoon shells and degummed fibers are presented in Tables I and II, and

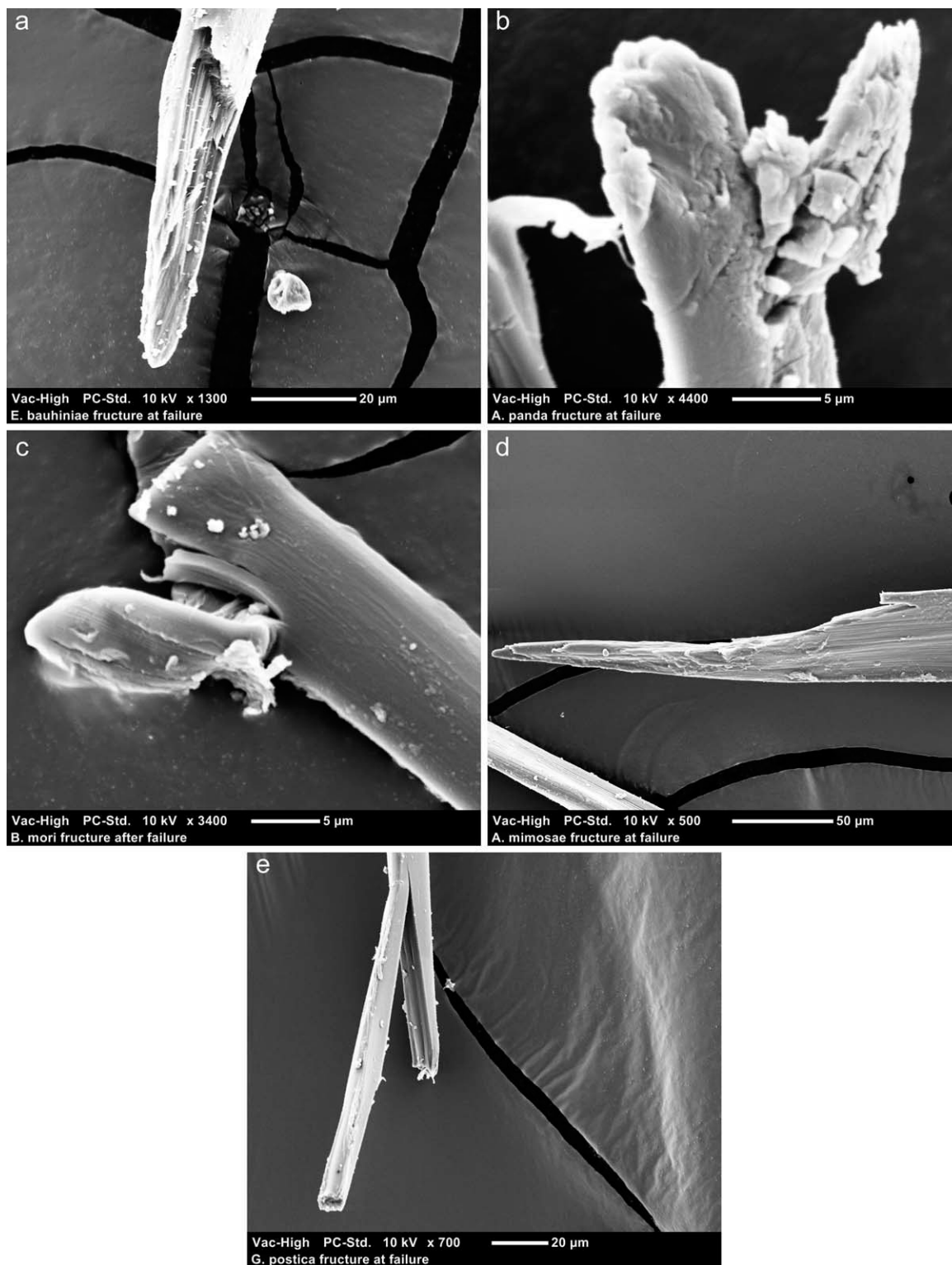


**Figure 3.** SEM micrographs of fracture surfaces of degummed fibers after tensile failure.

the average stress strain curves are presented in Figure 1(a,b). The results showed that the tensile properties of silk cocoon shells and degummed fibers differ between the species. For the cocoon shells, modulus reduced as strain increases and the binding points between fibers were observed to break

gradually. After a peak stress, there was rapid fall in stress, which indicated the continuous fiber bonding present in the cocoon shell that was wrecked, and simple entangled fibers were remained [Figure 1(a)]. *B. mori* cocoon shells had significantly higher maximum stress (101 MPa) and breaking

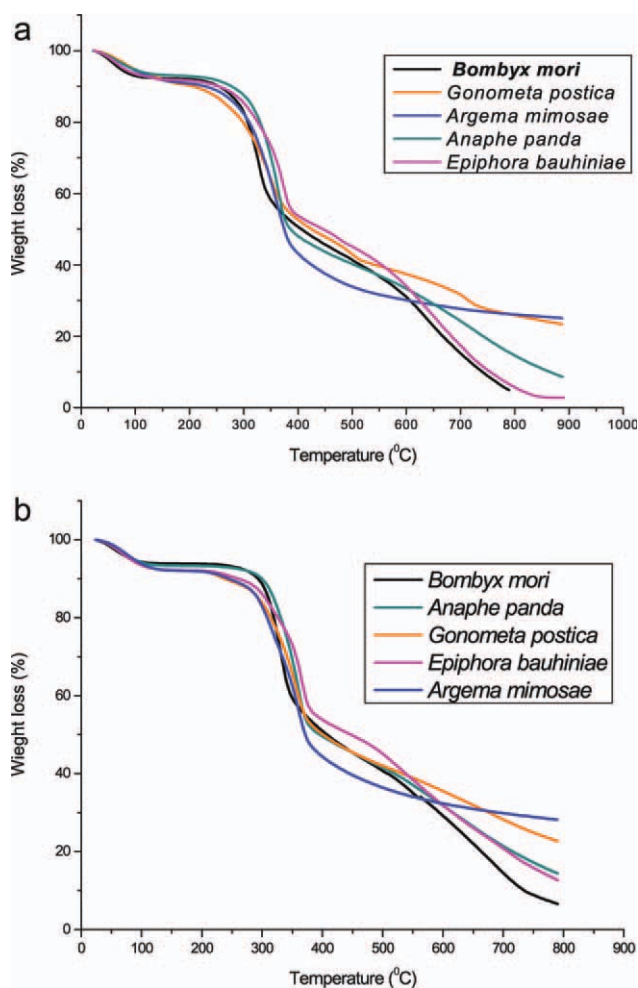


**Figure 4.** TGA curves cocoon shells and degummed fibers. [Color figure can be viewed in the online issue, which is available at [wileyonlinelibrary.com](http://www.wileyonlinelibrary.com).]

energy ( $20.1 \text{ J/cm}^3$ ). However, the wild cocoon shells had higher initial modulus and strain at maximum stress, though the values were not statistically significant (Table I).

Figure 1(b) shows that *B. mori* and *A. panda* fibers started with an elastic region followed directly by strain hardening where the stress increases nonlinearly with strain. The stress–strain curves of *A. mimosae*, *E. bauhiniae*, and *G. postica* fibers showed sig-

moidal shape, and an initial linear elastic region, yield region, and hardening regions were distinguished. *G. postica* fibers had the highest breaking energy ( $76.4 \text{ J/cm}^3$ ) and breaking strain (41.3%), whereas *E. bauhiniae* had the lowest breaking strain (247.7 MPa; Table II). *B. mori* had the highest breaking stress than the wild silk fibers (427.6 MPa), though it was not statistically significant with *A. panda* and *A. mimosae*. Despite the average cross-sectional area used to calculate the tensile properties, wild silk fibers showed noticeably higher standard deviation than *B. mori* indicating the considerable variation in the diameter of the fibers along their length and between fibers (Table III).

Fracture surfaces of the cocoon shells and single fibers were observed under SEM (Figures 2 and 3). Fiber debonding was observed after the tensile failure in all the species tested. Fibers of the cocoon shells were either broken or pulled out. *B. mori* and *G. postica* cocoons exhibited fiber pull-out. Detachment of the fibers was predominant in fracture surfaces with fairly clean and recognizable fiber surface without matrix adherence [Figure 2(a,c)]. *A. mimosae* cocoon shells were broken with a clear evidence of brittle failure, and few fibers were present holding the cocoon [Figure 2(b)]. *B. mori* and *A. panda* fibers seem to store the stress by stretching and then fail all at once [Figure 3(b,c)]. However, the rest of the fibers were without such process under stress and fracture smoothly. This appears to reflect the difference in the strain–stress curves.

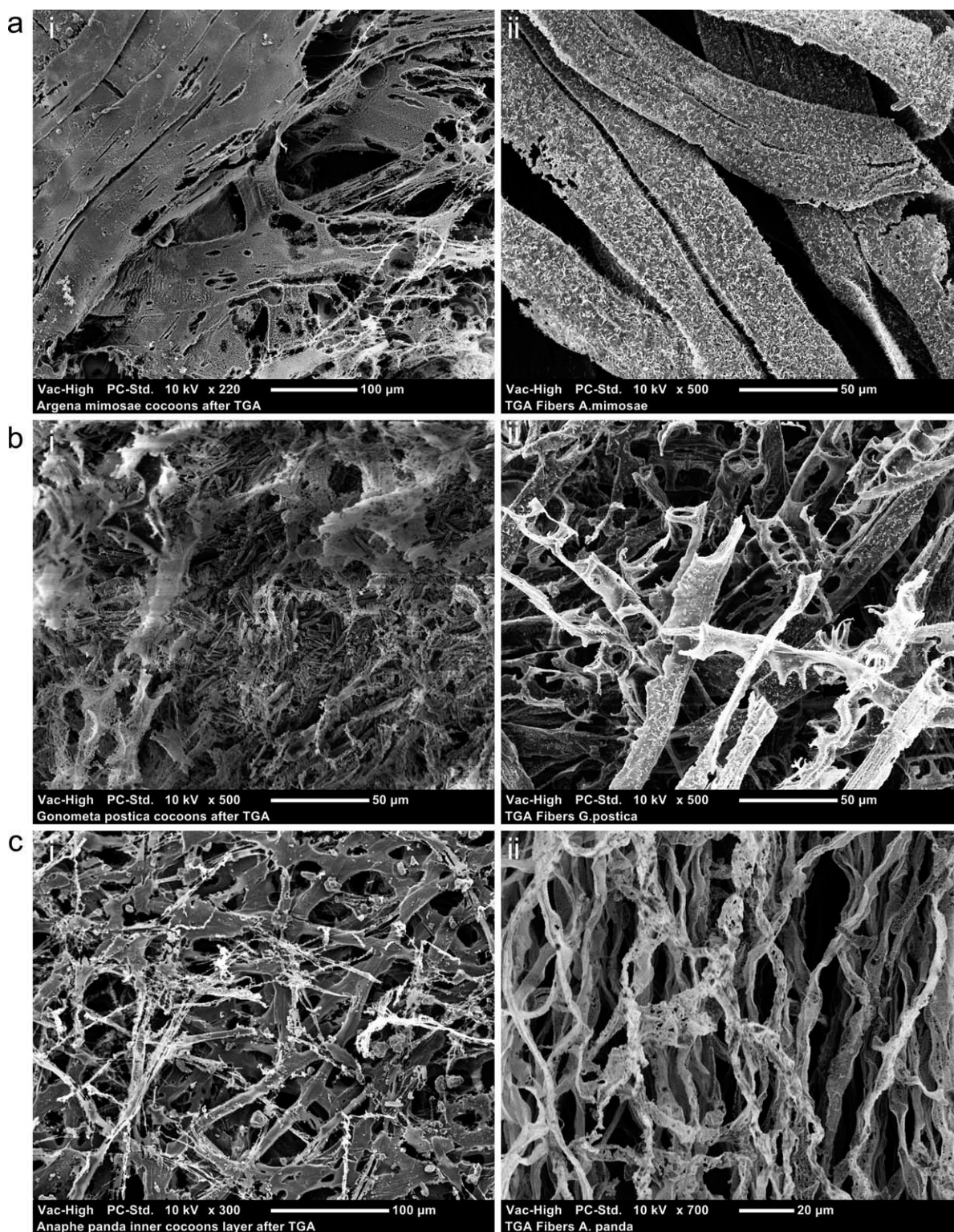
#### TGA

Figure 4(a,b) illustrates the thermal decomposition behavior of cocoon shells and degummed fibers, respectively. The TG curves showed that weight loss due to dehydration of absorbed water molecules associated with cocoon shells occurred rapidly up to 101, 120, 125, 154, and 127°C for *B. mori*, *G. postica*, *E. bauhiniae*, *A. mimosae*, and *A. panda*, respectively. The dehydration loss from cocoon shells was the highest for *A. mimosae* (11.9%) and the lowest for *B. mori* (9.8%) (Table IV). A substantial weight loss followed the gradual decrease in weight as heating temperature increased. Rapid weight loss begun at 296, 311, 302, 309, and 303°C for *B. mori*, *E. bauhiniae*, *A. mimosae*, *A. panda*, and *G. postica* cocoon shells, respectively [Figure 4(a)]. The thermal decomposition of *G. postica* cocoon shells occurred in more steps than the rest of the species with rapid decompositions occurring at temperature ranges of 483–506 and 710–730°C. *A. mimosae* TGA curve showed that the cocoon

**Table IV.** Weight Loss of Degummed Fibers and Cocoon Shells after TGA

Species	Dehydration (%)		Decomposition (%)		Total weight loss (%)	
	Cocoon shells	Fibers	Cocoon shells	Fibers	Cocoon shells	Fibers
<i>A. panda</i>	$9.9 \pm 0.5\text{b}$	$11.1 \pm 0.4\text{b}$	$52.0 \pm 0.1\text{b}$	$51.5 \pm 0.3\text{b}$	$91.3 \pm 0.1\text{b}$	$85.9 \pm 4.0\text{a}$
<i>A. mimosae</i>	$11.9 \pm 0.1\text{a}$	$12.8 \pm 0.0\text{a}$	$61.2 \pm 0.5\text{a}$	$59.2 \pm 1.9\text{a}$	$74.9 \pm 0.5\text{c}$	$71.8 \pm 1.0\text{b}$
<i>E. bauhiniae</i>	$11.8 \pm 0.1\text{a}$	$11.9 \pm 0.0\text{b}$	$46.5 \pm 0.3\text{d}$	$47.2 \pm 1.2\text{c}$	$97.2 \pm 0.1\text{a}$	$87.3 \pm 2.3\text{a}$
<i>G. postica</i>	$11.5 \pm 0.8\text{a}$	$13.3 \pm 0.4\text{a}$	$50.4 \pm 1.1\text{c}$	$53.1 \pm 1.4\text{b}$	$71.2 \pm 1.5\text{d}$	$77.3 \pm 3.4\text{b}$
<i>B. mori</i>	$9.8 \pm 0.1\text{b}$	$8.5 \pm 0.3\text{c}$	$49.5 \pm 0.2\text{c}$	$54.6 \pm 0.3\text{b}$	$95.1 \pm 0.4\text{a}$	$93.4 \pm 2.4\text{a}$

Means followed by the same letter in the same column are not statistically significant ( $P > 0.001$ ) according to LSD test.



**Figure 5.** SEM micrographs of cocoon shells (i) and degummed fibers (ii) after heat treatment.

shells attained constant weight after the rapid weight loss, whereas the rest of the species continued to lose weight gradually. *E. bauhiniae* and *G. postica* cocoon shells had the highest and the lowest total weight losses, 97.2 and 71.2%, respectively.

The TG curves in Figure 4(b) showed the weight loss from degummed fibers. Water loss from degummed fibers occurred rapidly up to 99, 109, 113, 105, and 109°C for *B. mori*, *E. bauhiniae*, *A. mimosae*, *A. panda*, and *G. postica*, respectively, which was then followed by further gradual weight loss. The total

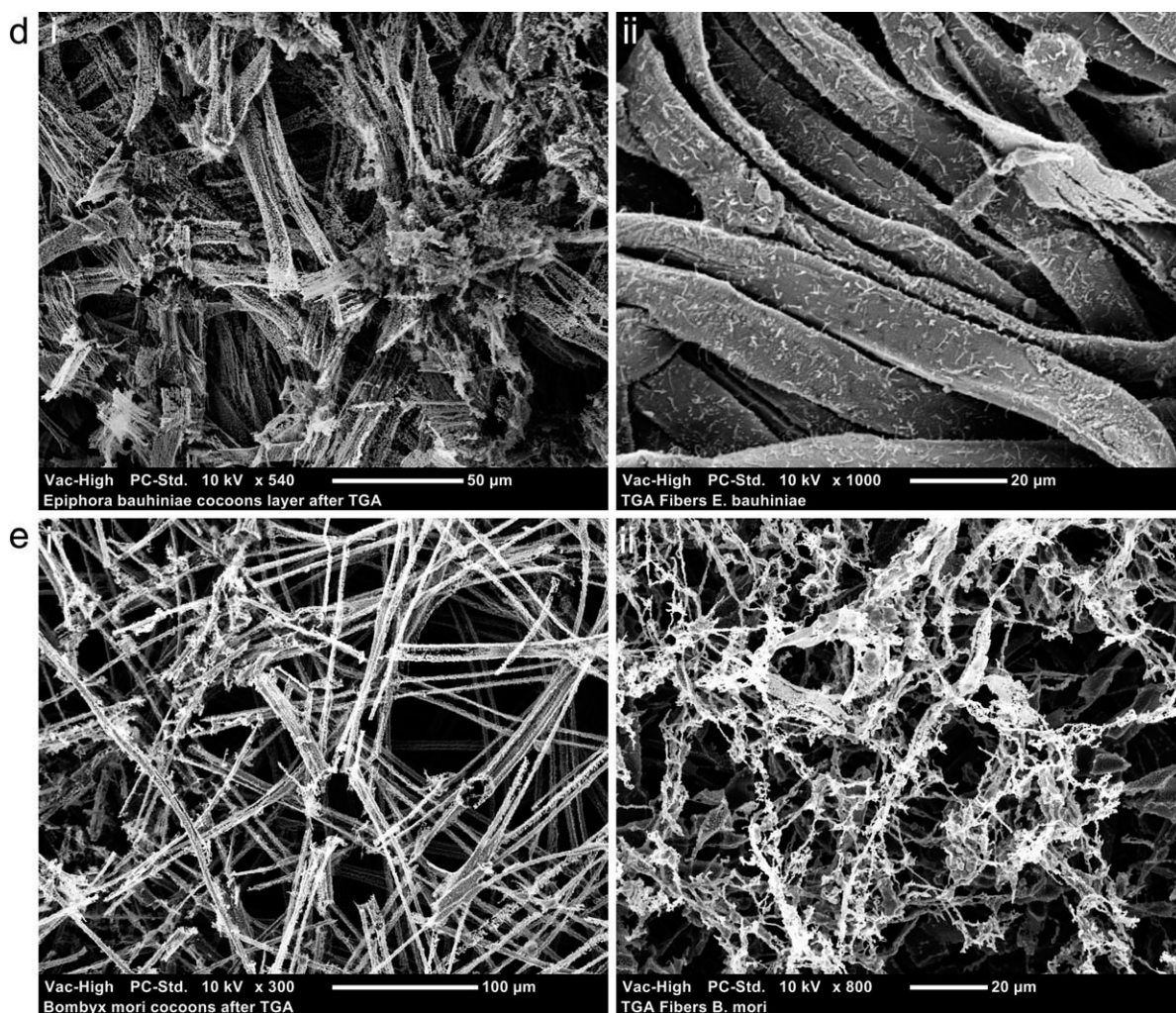


Figure 5. Continued.

dehydration loss was the highest for *G. postica* (13.3%) and the lowest for *B. mori* (8.5%) degummed fibers (Table IV). Major decomposition of degummed fibers commenced at 302, 290, 303, 312, and 305°C for *B. mori*, *E. bauhiniae*, *A. mimosae*, *A. panda*, and *G. postica*, respectively. The average onset decomposition temperature was higher for degummed fibers than the cocoon shells except for *A. mimosae* and *E. bauhiniae*. *A. panda* had the highest onset decomposition temperatures of 309 and 312°C for cocoon shell and degummed fibers, respectively. The multistep thermal degradation of *G. postica* cocoon shells could not be observed in degummed fibers. *B. mori* fibers had the highest total weight loss (93.4), though it is not significantly different from other species except *A. mimosae* and *G. postica*.

The SEM images showed that cocoon shells and degummed fibers maintained their shape in *A. mimosae*, *A. panda*, and *E. bauhiniae*, whereas *B. mori* and *G. postica* were completely decomposed and lost their structure in the process [Figure 5(a–e)]. In *A. mimosae* and *E. bauhiniae*, the broken individual fibrils became more evident and can be easily seen after the heat treatment.

## DISCUSSION

The results demonstrated the existence of distinct variations in the mechanical properties and in thermal degradation behaviors among the four African wild silk cocoon shells and degummed fibers. The stress–strain curves that are related to the applied stress to the resulting strain revealed that each species has its own unique stress–strain curve. This has previously been reported for mulberry and nonmulberry varieties.<sup>13,14</sup> *B. mori* and *A. panda* showed no well-defined yielding point and strain hardening region suggesting the presence of well-developed crystalline regions that are responsible for smaller and gradual elongation with increasing stress.<sup>15</sup> The study revealed that the African wild silk fibers have comparable mechanical properties to the commercial standard, *B. mori*. Sen and Babu<sup>15</sup> also reported that average breaking extension values are greater for nonmulberry varieties (21–24, 23–30, and 17–24% for Muga, Eri, and Tasar silk, respectively) than *B. mori* (12–15%). However, in our study, most of the wild silk fibers had lesser breaking elongation than *B. mori*. *Saturniidae* silk showed lower values of the elastic modulus and larger extensibility when compared with the *Thaumetopoeidae*, which is also found to be

true in our study.<sup>16</sup> In most of the results, the wild silk fibers showed nonsignificant difference in the measured tensile properties. The fracture properties of silk fibers are poorly reproducible and governed by microstructural defects rather than by intrinsic limitations of the silk polymer.<sup>17</sup> The morphological defects such as partial silk fibroin rupture observed in *G. postica* fibers can also be a possible cause for the drop of the tensile strength. The mechanical properties are also influenced by the fiber denier.<sup>18</sup> The tensile strength of the fibers is also attributed to the extent crystalline region with highly ordered structures and the ratio of other amino acids that confer elasticity in the amorphous domains.

The typical silk from *B. mori* cocoon has a tensile strength of about 0.5 GPa, breaking strain of 15–22%, and tensile elastic modulus 7–17 GPa.<sup>19,20</sup> Thus, for *B. mori*, the present findings match consistently with previous results. However, other studies reported that tensile modulus and the tensile strength of the normal compact cocoon are about 0.66 GPa and 53.98 MPa, respectively.<sup>21</sup> Zhao et al.<sup>22</sup> also reported comparable tensile modulus and breaking strain results for *B. mori* compact cocoon shells tested along longitudinal directions. However, they reported lower tensile stress (20 MPa). The variation in the measured data for cocoon shells might be attributed to several reasons. The irregular silk fiber arrangement and wrinkles throughout the cocoon shells that are related to the environmental conditions during cocoon formation and drying together with variation in cocoon thickness, and the entire spinning process contribute to the observed differences. The main reason for poor mechanical properties in cocoon shells of *G. postica* might be due to the presence of calcium oxalate crystals combined high gum contents leading to easy rupture and weak bonding between the fibers as can be evidenced from the SEM micrographs.

The study further showed that permanent decomposition of cocoon shells and fibers started very early for *B. mori* making the African wild silk fibers thermally relatively more stable. The wild cocoon shells had significantly higher temperature for dehydration, which suggests the presence of highly adsorbed water molecules (intrinsic structural water) and the variation in chemical composition of constituent proteins. The high heat stability of the cocoon shells proved their contribution as self-thermoregulation structures, and they will not be exposed to severe dehydration except under extreme environmental condition. In previous studies, similar results were reported for *B. mori* cocoon shells exhibiting dehydration and decomposition losses at 98 and 280°C, respectively.<sup>23</sup> They also suggested that the substantial weight decrease thought to be due to oxidation and cleavage reaction of the —OH chain of the silk fibers. The multistep decomposition of *G. postica* cocoon shells could be due to the presence of calcium oxalate crystals on their surface. *A. pernyi* silk fibers and other silks belonging to the family Saturniidae also undergo several steps of decomposition due to the difference in polymorphs of crystalline structure and amino acid composition.<sup>24</sup> The absence of change in structure of *A. mimosae* and *E. bauhinae* fibers

after thermal treatment might be due to the compactness of the fiber disks during the sample preparation process. In conclusion, the study confirmed that silks produced by the African wild silkmoths have properties that have considerable promise for commercial applications. Although *B. mori* and the wild silks are both class of natural proteins, their overall properties are different. The molecular structure, weight, and percentage crystallinity seem to play a role in distinctly different properties of the silks.

## ACKNOWLEDGMENTS

Thanks are due to *icipe*-African Insect Science for Food and Health for providing logistical and research support. The authors are highly indebted to Dr. Chris Holland, Ms. Fujia Chen, Dr. Tom Ghyesens, and other members of the Oxford Silk Research Group for their help, technical support, and expert suggestions. Funding was provided for Addis Teshome by the DAAD and for Fritz Vollrath by ERC (SP2-GA-2008-233409) and the AFOSR (F49620-03-1-0111).

## REFERENCES

- Zhao, H. P.; Feng, X. Q.; Cui, W. Z.; Zou, F. Z. *Eng. Fract. Mech.* **2007**, *74*, 1953.
- Chen, X.; Shao, Z. Z.; Marinkovic, N. S.; Miller, L. M.; Zhou, P.; Chance, M. R. *Biophys. Chem.* **2001**, *89*, 25.
- Shao, Z. Z.; Vollrath, F. *Nature* **2002**, *418*, 741.
- Manjunatha, H. B.; Rajesh, R. K.; Aparna, H. S. *J. Insect Sci.* **2010**, *10*, 1.
- Zhang, Y.; Yang, H.; Shao, H.; Hu, X. *J. Biomed. Biotechnol.* **2010**, *1*, 1.
- Lin, Z.; Huang, W.; Zhang, J.; Fan, J.; Yang, D. *Proc. Natl. Acad. Sci. U. S. A.* **2009**, *106*, 8906.
- Jiang, P.; Liu, H.; Wang, C.; Wu, L.; Huang, J.; Guo, C. *Mater. Lett.* **2006**, *60*, 919.
- Ki, C. S.; Kim, J. W.; Oh, H. J.; Lee, K. H.; Park, Y. H. *Int. J. Biol. Macromol.* **2007**, *41*, 346.
- Sutherland T. D.; Young, J.; Weisman, S.; Hayashi, C. Y.; Merritt, D. *J. Annu. Rev. Entomol.* **2010**, *55*, 171.
- Danks, H. V. *Eur. J. Entomol.* **2004**, *101*, 4333.
- Hans G. W.; McKarns, T. *Thermochim. Acta* **1990**, *169*, 1.
- Perez-Rigueiro, J.; Viney, C.; Llorca J.; Elices, M. *J. Appl. Polym. Sci.* **1998**, *70*, 2439.
- Das, S.; Chattopadhyay, R.; Gulrajani, M. L.; Sen, K. *Autex Res. J.* **2005**, *5*, 81.
- Rajkhowa, R.; Gupta, V. B.; Kothar, V. K. *J. Appl. Polym. Sci.* **2000**, *77*, 2418.
- Sen, K.; Babu, M. K. *J. Appl. Polym. Sci.* **2004**, *92*, 1098.
- Lucas, F.; Shaw, J. T. B.; Smith, S. G. *J. Textile Inst.* **1955**, *46*, 440.
- Perez-Rigueiro, J.; Viney, C.; Llorca, J.; Elices, M. *J. Appl. Polym. Sci.* **2000**, *75*, 1270.
- Iizuka, E.; Kawano, R.; Kitani, Y.; Okachi, Y.; Shimizu, M.; Fukuda, A. *Indian J. Seric.* **1993**, *32*, 27.



19. Hakimi, O.; Knight, D.; Vollrath, F.; Vadgama, P. 2007. *Compos. B: Eng.* **2007**, 38, 324.
20. Gosline, J. M.; Guerette, P. A.; Ortlepp, C. S.; Savage, K. N. *J. Exp. Biol.* **1999**, 202, 3295.
21. Huang, S. Q.; Zhao, H. P.; Feng, X. Q.; Cui, W.; Lin, Z.; Xu, M. Q. *Acta Mech. Sin.* **2008**, 24, 151.
22. Zhao, H. P.; Feng, X. Q.; Yu, S. W.; Cui, W. Z.; Zou, F. Z. *Polymer* **2005**, 46, 9192.
23. Zhang, H.; Magoshi, J.; Becker, M.; Chen, J. Y.; Matsunaga, R. *J. Appl. Polym. Sci.* **2002**, 86, 1817.
24. Kweon, H. Y.; Um, I. C.; Park, Y. H. *Polymer* **2000**, 41, 7361.